ARTICLE IN PRESS

Nuclear Engineering and Technology xxx (xxxx) xxx

Contents lists available at ScienceDirect

Nuclear Engineering and Technology

journal homepage: www.elsevier.com/locate/net

Original Article

# PARs interaction with in-containment safety systems during severe accidents in Western PWR containments

Joan Fontanet *, Luis E. Herranz

*Centro de Investigaciones Energéticas Medioambientales y Tecnológicas (CIEMAT), Unit of Nuclear Fission, Av. Complutense 40, Madrid, E-28040, Spain*

A R T I C L E I N F O

*Keywords:*
PARs
Combustible gases
Accident management
Simulation

A B S T R A C T

The combustion of flammable gases, such as hydrogen ($H_2$) and carbon monoxide (CO), during severe accidents in Light Water Reactors might threaten the containment integrity. In this context, the AMHYCO project, funded by the European Commission, aimed to enhance the understanding of combustion risks in Pressurized Water Reactors and assess accident management strategies. The presented study, conducted within AMHYCO, uses the integral code MELCOR v2.2 to systematically analyse the combined role of Passive Autocatalytic Recombiners (PAR) and safety systems in mitigating combustion risks. The $H_2$ and CO evolution is simulated in two reference scenarios for a generic 1000 MWe Pressurized Water Reactor: a Large Break Loss of Coolant Accident (LBLOCA) and a Station Black-Out (SBO). Results show that PARs effectively reduce flammable gas concentrations, though their performance depends on accident conditions. In low-steam scenarios and early vessel failure, such as a LBLOCA, combustible gas accumulation poses a significant challenge, especially during the ex-vessel phase. In these scenarios, reducing the containment cooling capacity has advantages for the combustion risk without affecting PAR's recombination capacity. Nonetheless, if pressure approaches the design pressure, reducing it might be a priority. In contrast, high steam concentration in SBO dilutes flammable gases, lowering combustion risk. The study quantifies the impact of spray-system recovery time, highlighting the importance of delaying activation timing so that PARs deplete enough combustible gases and oxygen to prevent deflagrations. These findings emphasize the need for specific accident management strategies to optimize PAR operation and cooling systems.

## 1. Introduction

In the evolution of a severe accident in a Light Water Reactor (LWR), hydrogen ($H_2$) can be generated by steam reaction with overheated zirconium and stainless steel in the Reactor Pressure Vessel (RPV). Moreover, in case of RPV failure, molten material might fall into the cavity and interact with the concrete (ex-vessel phase of the accident). The thermal decomposition of the concrete will produce steam and $CO_2$ that, when bubbling through the molten material, will result in further generation of $H_2$ and CO by oxidation of the metals remaining in the corium. The amount of combustible gases generated depends on the corium and concrete composition. The accumulation of $H_2$ and CO in the containment might form a flammable cloud that could threaten containment integrity and safety system components. Such energetic phenomena happened in the containment of TMI-2 [1] and in the reactor buildings of Units 1, 3 and 4 at the Fukushima-Daiichi Nuclear Power Plant [2].

Combustible gas hazards in nuclear power plants have been studied for a long time. Substantial effort has been made internationally to synthesise up-to-date knowledge on analyses related to hydrogen and carbon monoxide generation, distribution, combustion as well as mitigation measures [3–5]. Given hydrogen's safety relevance and the lack of knowledge, the combustion risk was ranked as a high-importance issue in the EURSAFE [6] project and, more recently, by the NUGENIA association [7]. Moreover, dynamic loads that threaten the containment integrity caused by deflagrations have become a key concern in nuclear safety. In particular, the post-Fukushima stress tests performed in Nuclear Power Plants (NPP) in the European Union highlighted the need to implement mitigation measures to prevent hydrogen explosion hazards [8]. The IAEA also defined the safety requirements and acceptance criteria for NPPs to ensure containment integrity in severe accident conditions [9]. Furthermore, to avoid excessive accumulation of combustible gases and to prevent potential uncontrolled combustion, Passive Autocatalytic Recombiners (PARs) are an effective mitigation

* Corresponding author.
*E-mail addresses:* joan.fontanet@ciemat.es (J. Fontanet), luisen.herranz@ciemat.es (L.E. Herranz).

https://doi.org/10.1016/j.net.2026.104483
Received 23 December 2025; Received in revised form 1 May 2026; Accepted 8 June 2026
Available online 9 June 2026


Please cite this article as: Joan Fontanet, Luis E. Herranz, *Nuclear Engineering and Technology*, https://doi.org/10.1016/j.net.2026.104483

measure against hydrogen and carbon monoxide hazards [5,10].

In this context, the AMHYCO project [11] was launched in 2020 under the coordination of the UPM (Universidad Politécnica de Madrid) and with the funding of the European Union. The main objective of the project was to extend the understanding of $H_2$ and CO combustion risk that supports an optimization of accident management measures in the present Pressurized Water Reactors (PWR). A workpackage (WP4) of the project was devoted to conducting a comprehensive analytical assessment regarding the $H_2$ and CO combustion risk and the interactions between the mitigation measures (PAR) and safety systems (venting, sprays, or fan coolers) in different generic PWR containments [12]. Within this workpackage, CIEMAT performed a set of simulations with MELCOR v2.2 [13] in a generic containment representing a 3-loop Westinghouse PWR-1000 MWe reactor.

The MELCOR code and other lumped-parameter (LP) codes compute fluid properties as volume average within a given control volume and therefore tend to amplify mixing in a necessarily coarse nodalization. In addition, inter-compartment flows are affected by these volume-averaged properties. In this context, users must be aware that the results will not provide local details but global trends. Nonetheless, MELCOR has been used in containment interpretation of several experiments, which have allowed the validation of its model for hydrogen mitigation [14–16]. MELCOR has also been used, together with other LP codes, in benchmark exercises such as those defined in the SARNET project in plant application [17]. Moreover, in recent years, MELCOR has been used by several international organizations for the simulation of hydrogen behaviour in different types of nuclear power plants: PWR [18–20] or VVER [21]. MELCOR can then provide valuable results about the PARs' performance in combination with other safety systems. However, fewer publications used MELCOR-based PAR modelling to derive accident management-oriented insights on the time-dependent interaction of PARs and other containment systems.

The objective of this paper is to systematically assess how in-containment safety systems interact with PARs and how these interactions affect their efficiency in removing combustible gases during both in- and ex-vessel phases of a severe accident, as well as the resulting impact on the containment atmosphere's flammability margin. For a detailed analysis of accident management, two sequences are selected: a LBLOCA (Large Break Loss of Coolant Accident) and a SBO (Station Black-Out) [22,23]. These scenarios represent, respectively, low-steam and high-steam conditions, which strongly influence the combustion risk. The main insights from this analysis focus on the operation conditions, steam dilution, oxygen depletion, and pressure control.

## 2. Approach and model

### 2.1. Approach

The basis of the sequence analysis in the AMHYCO project [12] is the extension of the generic containment model methodology developed in the SARNET-II project [17] to different PWR containment designs. To meet the objectives of the AMHYCO project, the generic containment model must be built up from publicly available data [24] and the boundary conditions and nodalization must be determined precisely. This methodology uses LP codes to simulate the full plant for different sequences to determine the fluid releases and heat exchanges within the containment atmosphere, as well as the initial conditions. These data are then used to define external sources in the generic containment stand-alone model by appropriate data files.

Based on this model, CIEMAT has built up the MELCOR v2.2 dataset for the generic Westinghouse PWR containment. The mass and energy sources defined in AMHYCO are then treated as external sources in the MELCOR containment model. Besides, the heat transfer from the molten corium in the cavity is set as a direct heat source into the cavity atmosphere. Fission products, and therefore their associated heat, are considered in the simulations. Boundary condition data for the LBLOCA sequence have been obtained from the simulations performed by CIEMAT, whereas the SBO simulations have been carried out by IRSN, also as part of the project [22,23].

### 2.2. Containment nodalization

The total internal free volume of $\sim 6.1 \cdot 10^4$ m$^3$ is represented by 11 different control volumes (Fig. 1) with an additional large volume to model the environment. A total of 32 flow paths are defined to model the gas flows between these volumes. The flow path lengths are defined as the center-to-center distance between volumes. This definition follows the guidelines in the MELCOR's manual [13]. Finally, the model considers 71 heat structures that capture the total heat capacity and heat transfer area of all concrete and steel containment surfaces.

Concrete properties are taken from literature for representative high-density concrete (2500 kg/m$^3$). Because steam condensation promotes the combustion risk, the concrete thermal conductivity, λ, as a function of the concrete temperature $T$, is set to the upper limit in EUROCODE [25],

$$\lambda = 2 - 0.2452\left(\frac{T}{100}\right) + 0.0107\left(\frac{T}{100}\right)^2 \mathrm{W} \Big/ \mathrm{m{\cdot}K}$$

which is significantly higher than MELCOR's default value of 0.93 W/m·K [13]. It is worth noting that if the simulation interest were focused on the rise in containment pressure, the lower limit on thermal conductivity would give more conservative results.

The BURN package of MELCOR, devoted to simulating the combustion of gases, is not activated since one of the aims of this work is to explore the possible accumulation of combustible gases and their removal by PARs without being affected by possible deflagrations.

### 2.3. PARs model

PAR's efficiency to recombine $H_2$ by reacting with $O_2$ is modelled using control functions based on the Framatome correlations for recombination mass rates [26,27]. These correlations have been extended within the AMHYCO project to conditions with low oxygen concentration and/or significant CO fraction, such as those found in the ex-vessel phase of a severe accident. The general expression for the recombination rates of PARs can be written as:

$$R_{H2} = \eta_{H2} \cdot \left(k_1 \cdot P + k_2\right) \cdot C_{off} \tag{1}$$

$$R_{CO} = \eta_{CO} \cdot \left(k_1 \cdot P + k_2\right) \cdot C_{off} \tag{2}$$

where $\eta_{H2}$ and $\eta_{CO}$, are the effective $H_2$ or CO concentration for recombination. $P$ is the pressure and $C_{\text{off}}$ is the cut-off condition. Finally, $k_1$ and $k_2$ coefficients depend on the PAR dimensions. Details of these expressions are given in the paper by Braun and Reinecke [28].

The only system considered for combustible gas depletion is PARs and no thermal recombiner or igniters are considered in this work. A total of 40 PARs of two different sizes, FR-1500T and FR-960, are distributed in the containment as detailed in Table 1 [24].

## 3. Sequences description

Two accident sequences are simulated: LBLOCA and SBO. These sequences were selected within AMHYCO for their relevance to containment integrity [22,23]. Both have very different characteristics that make them of interest. The first one, LBLOCA, evolves with a relatively low containment steam concentration, and consequently, so does the pressure, while the fraction of combustible gases is significant. In contrast, SBO evolves with high vapour content and high pressure, while the combustible gas fraction is moderate. In none of the sequences does the pressure reach sufficiently high levels to require the activation of the FCVS (Filtered Containment Venting System).

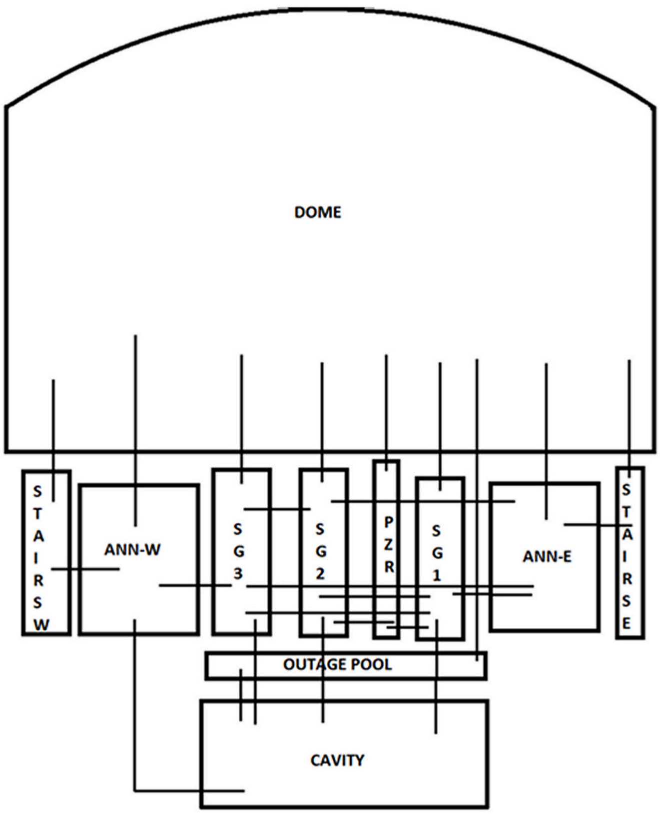


**Fig. 1.** Containment nodalization.

The LBLOCA is initiated by a double-ended guillotine break in the hot leg of the pressurizer's loop. Therefore, water and steam are discharged into the containment almost immediately (t = 0.003 s) in the SG1 compartment (Table 2). Hydrogen generation due to core degradation begins at 1200 s. Later in the sequence, the RPV fails early in the sequence (t = 2.4 h), and the ablation of the limestone concrete in the cavity initiates at 2.6 h with the subsequent generation of $H_2$ and CO by Molten Corium-Concrete Interaction (MCCI).

For the LBLOCA base case, sprays are automatically activated early in the transient due to a high-containment pressure signal. The activation setpoint is 2.6 bar to sprinkle water into the dome at a constant flow rate of 0.208 $m^3$/s. The initial spray water is supplied from the external RWST (Refueling Water Storage Tank) at 30 °C. When the RWST inventory is depleted (approximately 2.1 h after injection stars), the spray system switches to recirculation mode, taking water from the containment sump. To model the heat exchanger's effect during recirculation operation, the water injection temperature is set to 30 °C below the sump temperature.

Due to the loss of electrical power in the SBO, none of the in-containment safety systems are available at the beginning of the sequence. The overpressure in the reactor coolant system is relieved through the pressurizer safety valves towards the PRT (Pressurizer Relief Tank). The $H_2$ produced by the cladding oxidation is also conducted to the PRT with the steam. When the PRT rupture disk breaks at t = 2.4 h, steam, and later also $H_2$, are discharged into the containment's annular-east (ANN-E) compartment (Table 2). After this event, the release from the primary circuit is regulated by the pressurizer's safety valves. The first $H_2$ release into the containment is produced at t = 3.81 h. The RPV fails at t = 11.58 h, and the concrete decomposition starts in the cavity at t = 11.60 h. In this sequence, siliceous concrete is assumed in the cavity. Table 2 summarizes the chronology of the main events in the sequences.

Different cavity concrete compositions were intentionally selected in the two base sequences to span contrasted MCCI gas-production regimes relevant to $H_2$/CO combustion risk and PAR performance. The LBLOCA base case assumes limestone concrete to represent CO-richer MCCI under low-steam conditions, which is particularly challenging for PARs in the ex-vessel phase. The SBO base case assumes siliceous concrete to provide a complementary, more $H_2$-promoting MCCI regime under high-steam conditions. Finally, the sensitivity effect with the concrete composition is also analysed (section 4.2.3) to explicitly assess the impact of increased CO generation and $H_2$/CO competition on PAR efficiency, particularly under spray-recovery conditions.

Starting with the base case for each sequence, sensitivity calculations are performed to analyse the effect of different safety system actuations on the evolution of combustible gas clouds and their combined impact with PARs.

## 4. Results

### 4.1. Large break LOCA (LBLOCA)

The LBLOCA is characterized by an initial sudden rise in containment pressure at the beginning of the transient, driven by rapid water-steam discharge. As a direct consequence, the containment spray system is automatically activated (Table 2). The main effect of the spray is a reduction in containment pressure through the condensation of steam on the water droplets. After about 2 h of operation, the sprays switch to recirculation mode, taking water from the containment sump and re-spraying it after it is cooled in the intermediate heat exchanger.

In this LBLOCA sequence, the discussion focuses on the dome compartment because the combined effects of thermal-hydraulic conditions of the gas release, containment layout, and sprays operation in the dome make it the most representative compartment regarding gas combustion.

The fast generation of $H_2$ in the in-vessel phase, but especially the sustained generation of $H_2$ and CO by MCCI in the ex-vessel phase, leads to the accumulation of combustible gases in the containment up to

**Table 2**
Sequence description and main events timing.

| | LBLOCA | SBO |
|---|---|---|
| Spray activation | 4.1 s | Not available |
| Sprays switch recirculation | 2.1 h | Not available |
| Containment fan coolers | OFF | Not available |
| Discharge compartment | SG1 | ANN-E |
| Fluids release | 0.003 s | 2.4 h |
| First $H_2$ release | 1200 s | 3.81 h |
| RPV failure | 2.4 h | 11.58 h |
| Onset of MCCI gases generation | 2.6 h | 11.60 h |

RPV, reactor pressure vessel; MCCI, molten core-concrete interaction; SG, steam generator; ANN-E, annular-east compartment; LBLOCA, Large Break Loss of Coolant Accident; SBO, Station Black-Out.

**Table 1**
PARs distribution inside the containment [24].

| | Cavity | SG-1 | SG-2 | SG-3 | Ann-E | Ann-W | PZR | Stairs-E | Stairs-W | O.P. | DOME |
|---|---|---|---|---|---|---|---|---|---|---|---|
| Volume ($m^3$) | 775 | 1469 | 1717 | 1906 | 3306 | 3458 | 411 | 111 | 218 | 1178 | 46744 |
| FR-1500 | - | 2 | 2 | 2 | 2 | 2 | - | - | - | - | 10 |
| FR-960 | 2 | 4 | 4 | 4 | - | - | 3 | 1 | 1 | 1 | - |

SG, steam generator; Ann, annular compartment; PZR, pressurizer compartment; O.P., outage pool; E, east; W, west.

flammability conditions [3,5], as shown in the Shapiro diagrams below. The low steam concentration resulting from spray operation means the steam dilution is insufficient to prevent the cloud from becoming flammable.

Finally, different sets of parametric cases are analysed to assess the impact of PAR recombination capability (section 4.1.1) and cooling system activations (section 4.1.2) on the containment atmosphere.

#### 4.1.1. Effect of PAR performance

In a severe accident, the catalytic plates of PARs could become contaminated by smoke, oils, or other organic substances and may partially lose their recombination capability. For this reason, three recombination efficiencies are considered to explore the effect of PAR's degradation: 100% (full capacity), 75% (degraded), 50% (severely degraded). The simulation without PARs is presented as a limiting case.

The impact of different PAR efficiencies on containment pressure and on the dome's temperature (Fig. 2) is overall small. PAR operation has two effects: the formation of steam by reacting $H_2$ and $O_2$ (with a net reduction in molar content) and the heating up due to the exothermic recombination reaction. The operating spray system mostly condenses the produced steam, thereby increasing the effect of reducing the number of moles in the containment atmosphere. Besides, the spray system also partially compensates for the heat released by the PARs.

Results show that PARs are effective, even with a "reduced efficiency", in avoiding conditions of uncontrolled combustion in the in-vessel phase. This is consistent with the recombination dependence on combustible gas concentration. Nonetheless, the assumed PAR system is insufficient to prevent flammability during the ex-vessel phase when CO and $H_2$ are generated and accumulated in the containment. This behaviour is due to the large generation of combustible gas after the onset of the MCCI. Due to the low steam concentration of this scenario, the gas mixture deeply enters the flammability region in the Shapiro diagram for the dome compartment (Fig. 3). In the long term, during the accident evolution, the steam and $CO_2$ generated by MCCI, once the corium gets completely oxidized, partially dilute the flammable cloud. This fact, combined with the prolonged operation of PARs, reduces the concentration of combustible gases, especially oxygen, making the containment atmosphere inert (Fig. 3).

#### 4.1.2. Effect of cooling systems

Besides the spray system, the PWR-W containments are equipped with fan coolers to provide the containment with suitable cooling. Fan coolers are activated automatically by a containment high-pressure signal (setpoint at 1.3 bar). The operation of fan coolers simultaneously with the failure of the spray's intermediate heat exchanger (HX) between the sump and the spray nozzles is postulated. Moreover, the total loss of cooling capacity in the recirculation mode is also considered (i.e., unavailability of the HX). Therefore, three different cases are considered:

- Sprays working as expected (i.e., with the HX in the recirculation mode).
- Unavailability of the HX (labeled as Sprays w/o HX in figures below).
- Unavailability of the HX with parallel operation of fan coolers (labeled as Sprays w/o HX + FC in figures below).

As long as the spray system draws water from the external RWST, the HX is not in use. Thus, significant deviations between these cases occur only after the spray system switches to recirculation mode. The simultaneous operation of fan coolers with the spray system in the injection mode leads to a very slight reduction of the pressure and temperature in the dome (Fig. 4). The evolution of the pressure and dome's temperature differs more after the start of the recirculation mode ($t > 2$ h). Without the HX, the water sprayed into the containment dome has the temperature of the water in the sump. Consequently, the spray system loses its efficiency due to steam condensation. The first effect is a fast rise in both pressure and temperature in the containment. At the conditions reached at about 2.5 h, fan coolers are able to keep up with the energy release from the core melt. Therefore, the pressure evolution follows the one for the normal spray operation, although moderately higher. The lack of any cooling system (no HX or fan coolers) causes the sprayed water temperature and the steam content to rise continuously and more rapidly than in the other two cases with heat removal (Fig. 4). Considering only the combustion risk, the most favorable case is the one without any cooling system for the containment (Fig. 5).

The cooling capacity of the containment (i.e., fan coolers and HX) hardly has any effect on the recombination rate by the PARs (Fig. 6). Indeed, the recombination correlation for both $H_2$ and CO (Eqs. (1) and (2)) depends basically on the partial pressure of each gas in the atmosphere surrounding the PAR and does not include a direct dependence on steam. The only noticeable effect of steam is a shorter cutoff time due to CO poisoning of catalyst plates at low $O_2$ concentrations. The higher the pressure (no heat exchanger), the lower the $O_2$ concentration, and the earlier the cut-off criterion for the PARs is reached.

### 4.2. Station Black-Out

In a SBO, the containment pressure starts rising when the pressurizer relief tank disk ruptures. At this instant ($t = 2.4$ h), the $H_2$-mixture accumulated in the PRT is released into the containment. After the disk rupture, communication between the primary system and the containment is primarily governed by the cycling of the pressurizer safety valves, which continue releasing steam to the containment in the annular-east compartment (ANN-E). Results and discussion are therefore reported in this compartment, since the initial accumulation of steam and combustible gases occurs there and represents the higher combustion risk.

Successive oxidation runaways and/or steam flashing in the reactor pressure vessel lead to the containment pressure and temperature steps observed between 2.4 and 10.5 h (Fig. 7). The temperature step at 10.5 has special significance and is driven by steam flashing as hot material falls into the lower plenum in the highly degraded core.

These pressure surges are followed by periods of pressure relaxation due to steam condensation on the containment walls. At 2.6 h, the pressurizer valves are maintained locked open for the rest of the accident. The decrease in pressure after 10.2 h is due to the end of steam release from the vessel, once the core is completely uncovered, together with the steam condensation on the walls. The vessel fails at 11.58 h at low pressure, and then the generation of gases by MCCI starts.

Due to the unavailability of safety systems, the SBO sequence is characterized by a significantly higher containment pressure than the LBLOCA sequences. From a combustion risk perspective, the high steam content of the containment atmosphere lowers the concentration of combustible gases. However, it is worth noting that, if combustion occurs, the high pressure might also challenge containment integrity. Moreover, a reestablishment of electric power is a realistic possibility in a SBO, and it could lead to a recovery of the spray system. The start of the spray system would then drastically change the flammability of the containment atmosphere. Spray actuation is considered in the recovery sensitivity cases.

#### 4.2.1. Effect of PAR performance

Similar to the LBLOCA sequence, PAR performance is analysed across different efficiencies. A simulation without PARs is also given for comparison. The different PAR recombination rates show only a slight effect on the containment pressure and annular-east temperature (Fig. 7). In the SBO, the capability of the containment to remove heat and/or steam is limited to the condensation on walls. Thus, during the in-vessel phase and the first hours of the ex-vessel phase, the energy release of the PARs contributes to containment pressurization and to a heat-up of the containment gas phase. Regarding combustion risk, PARs significantly recombine $H_2$ during the in-vessel phase, and when the

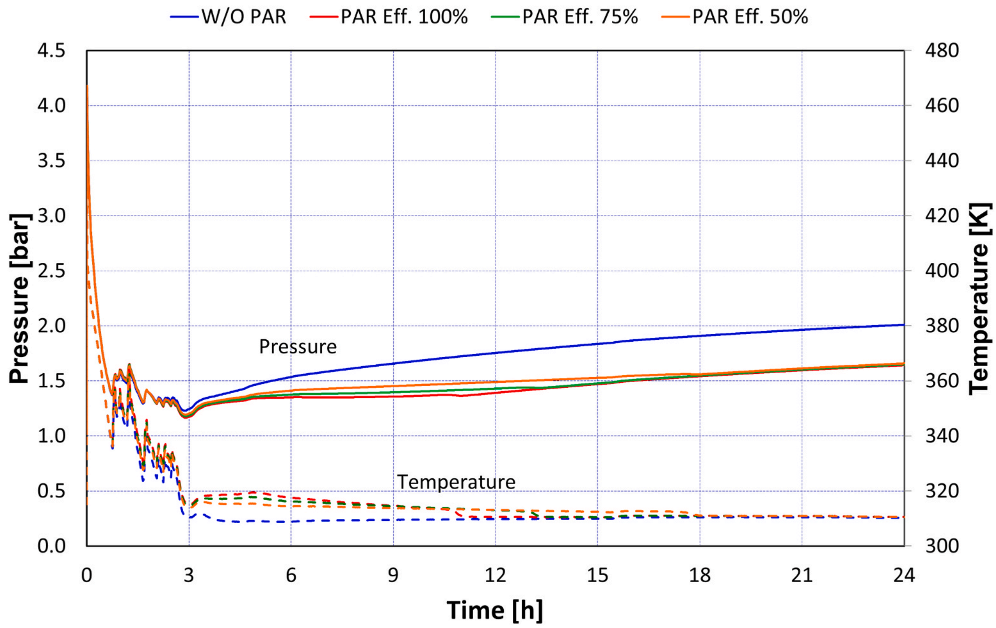


**Fig. 2.** Containment pressure and dome's temperature evolution for the LBLOCA sequence. Comparison of PAR's efficiency.

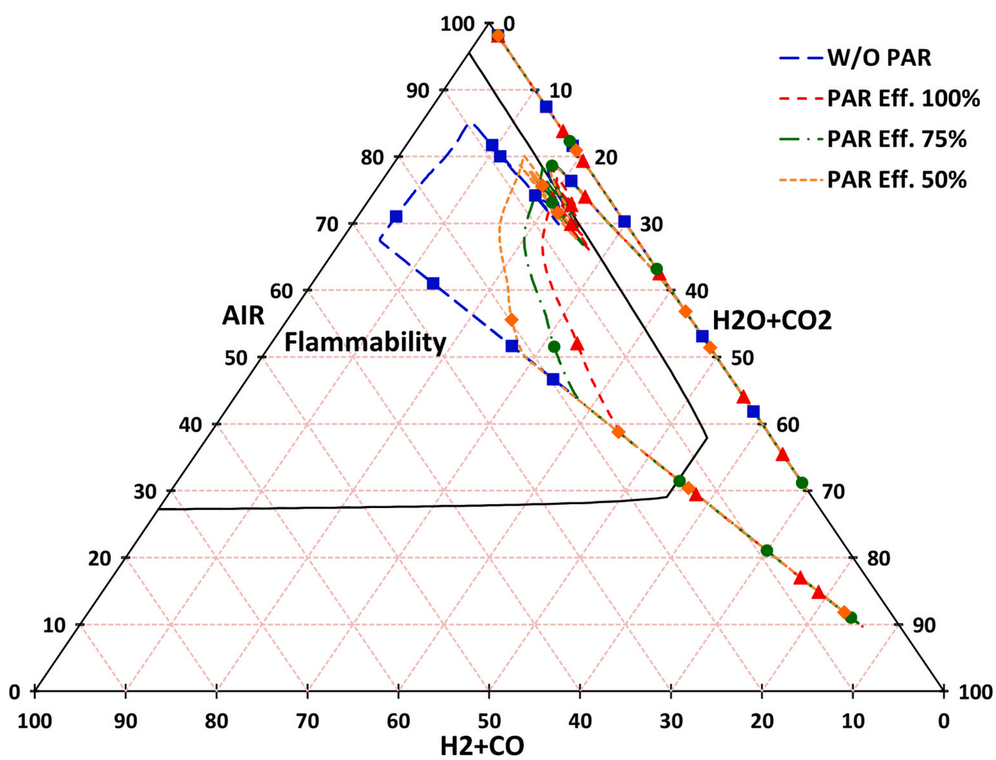


**Fig. 3.** Shapiro diagram in the dome for the LBLOCA. Comparison of PAR's efficiency.

combustible gases accumulate well into the ex-vessel phase, the atmosphere in the annular-east (ANN-E) compartment is inerted due to oxygen depletion (Fig. 8). Therefore, PARs drastically reduce the risk of uncontrolled flammability, even when assuming a degraded PAR efficiency.

*4.2.2. Effect of spray recovery time*

The late recovery of sprays in a SBO, although it has positive effects on pressure reduction, can cause a significant rise in the concentration of combustible gases because of the steam removal. Therefore, in a scenario with PARs, the time for spray recovery has a significant impact on the combustion risk. Based on the scenario with PARs at full efficiency, different scenarios are analysed considering four different times for the spray activation. The earliest time considered, 4.5 h since the onset of power loss, is when the evolution of this specific scenario leads to the entry into the severe accident management criteria [29,30]. For the successive scenarios, the spray activation is considered at 3-h intervals (i.e., 7.5 h, 10.5 h, 13.5 h). The figures below compare the sequence evolution for the base case without sprays (labeled 'w/o SPR') with the four spray activation times considered.

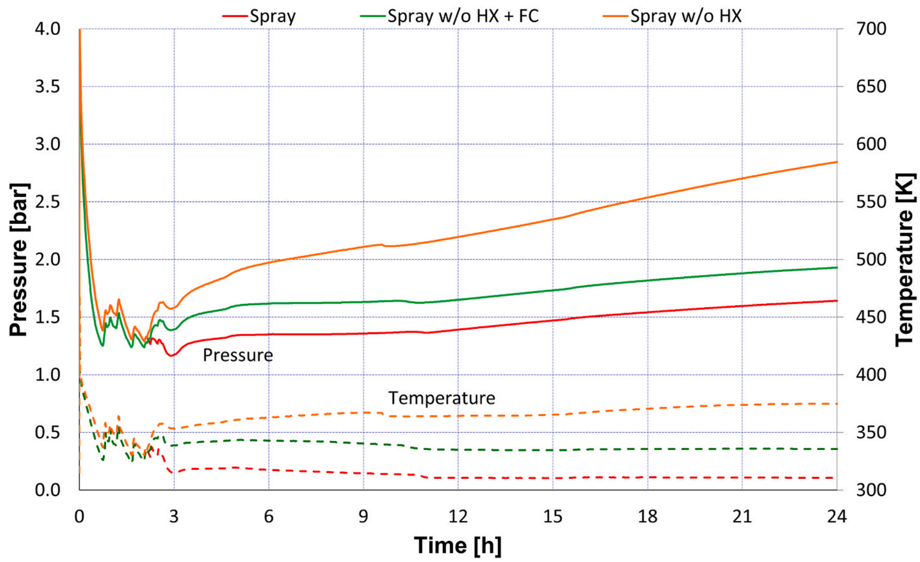


**Fig. 4.** Containment pressure and dome's temperature evolution for the LBLOCA sequence. Comparison of safety systems.

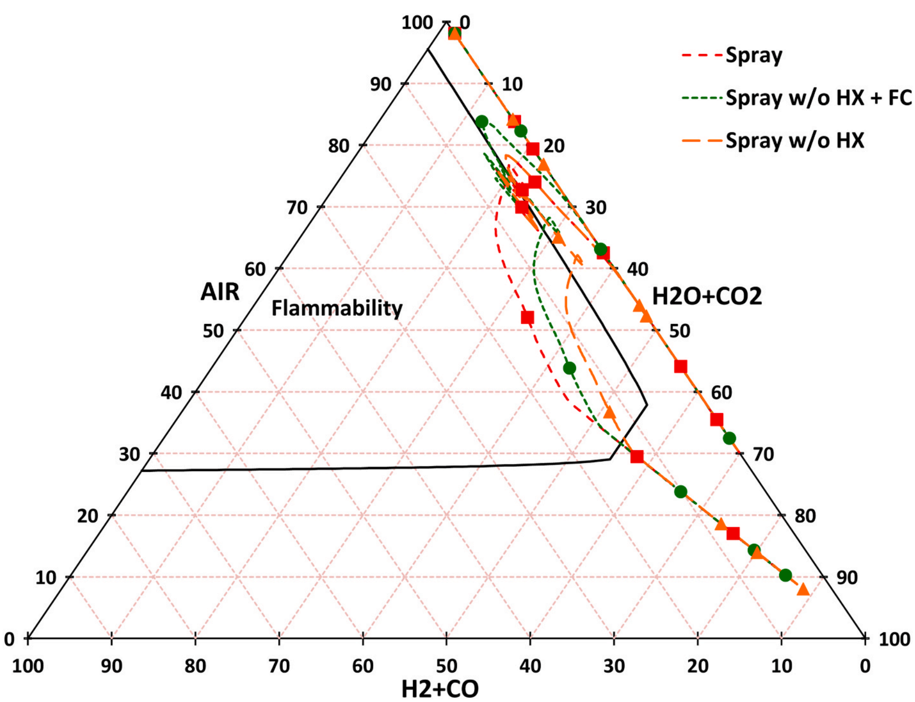


**Fig. 5.** Shapiro diagram in the dome for the LBLOCA sequences. Comparison of the containment cooling systems.

The spray system is able to reduce the containment pressure on the 1-h time scale (Fig. 9). With the spray system working, the diluting effect of steam vanishes, and the $H_2$ and CO molar fractions increase accordingly with the consequent risk of deflagrations in the annular-east compartment (Fig. 10). The parametric cases show that with the two earliest times considered (i.e., 4.5 and 7.5 h), the $H_2$ concentrations exceed the lower bound of the flammability limits (Fig. 10 (a)). During these periods, the PARs have not depleted enough oxygen yet to make the containment inert. A flammable cloud is not predicted for the two later times (10.5 and 13.5 h). At these times, PARs have already recombined enough hydrogen (and/or oxygen) to avoid flammable conditions even with the spray activation (Fig. 10 (b)). CO is not involved in this discussion, as only the latter time corresponds to the ex-vessel phase.

After a spray activation, the composition of the containment atmosphere changes drastically. Nonetheless, as discussed in the LBLOCA sequence effect on cooling systems, this does not lead to a strong impact on the recombination rate of the PARs (Fig. 11). The slight effect observed at 12 h in the last spray activation time is due to the cliff effect of the PARs cut-off. At about 12 h, $H_2$ concentration is very close to 2%, which is the setpoint for PARs cut-off at low combustible gas concentration.

#### 4.2.3. *Effect of concrete composition*

An important aspect when analysing combustion risk in the ex-vessel phase is the generation of CO by an ongoing MCCI. It is known that the CO generation depends directly on the concrete composition. Therefore, the same study concerning spray reactivation in a SBO case is repeated,

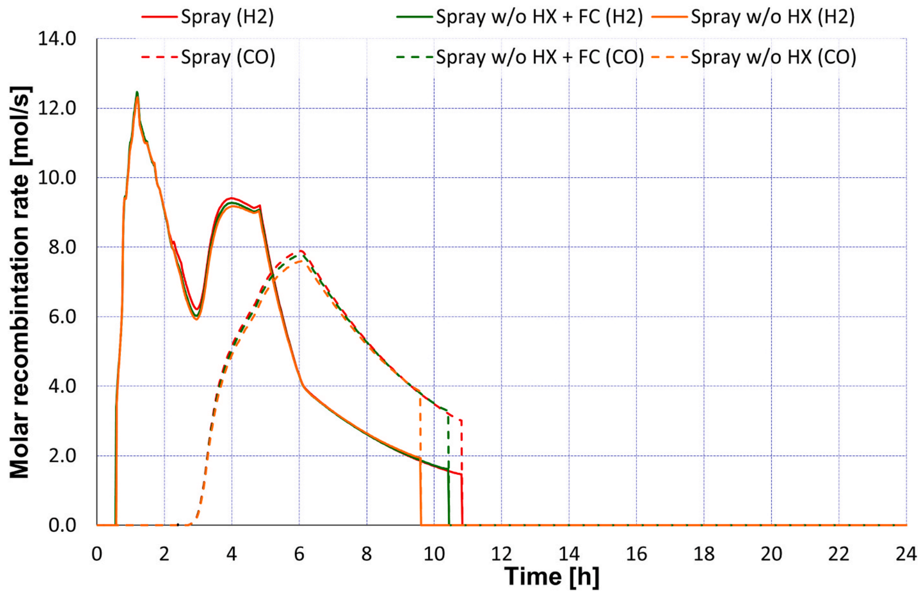


**Fig. 6.** Total PAR's recombination rate in the dome with different cooling systems for the LBLOCA sequence.

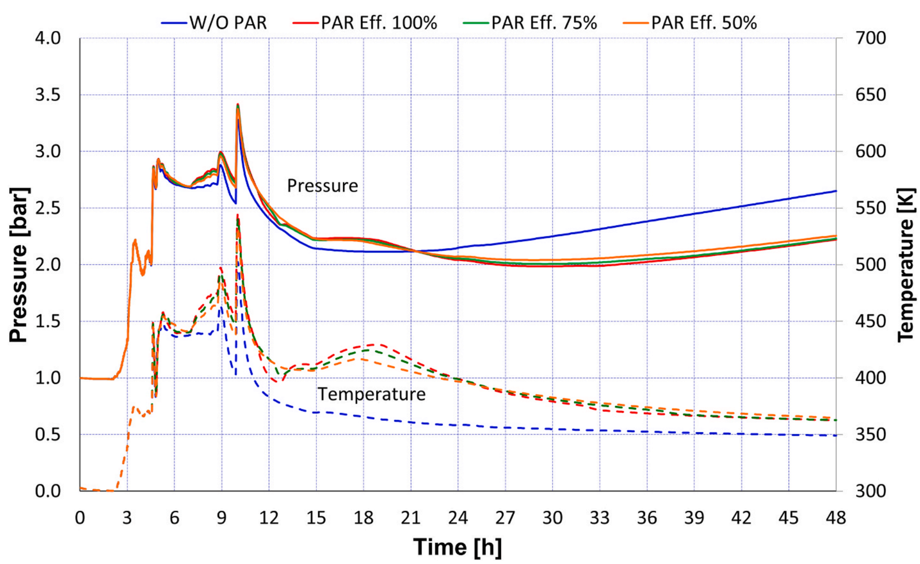


**Fig. 7.** Containment pressure and annular-east temperature evolution for the SBO sequence. Comparison of PAR's efficiency.

but assuming a limestone-type concrete instead of a silicious concrete. The analysis focuses on sequences with spray recovery due to their high impact on flammability risk. Therefore, the same spray recovery times as in section 4.2.2 are considered. Results show that for all the considered spray activation times, the presence of CO in the ex-vessel phase moves the combustible mixture to flammability before containment inertiation due to the low oxygen concentration (Fig. 12(a) and (b)). The competition between CO and $H_2$ for reaction on the catalytic surface, along with the lower efficiency of CO recombination compared to $H_2$, are the reasons for this outcome.

## 5. Conclusions

The basis of this work is a stand-alone model for a generic PWR-W containment that is fed with the initial and boundary containment conditions (i.e., mass and thermal energy input) from a LBLOCA and a SBO sequence. Through the LBLOCA scenario, insights into a low-pressure and low steam fraction scenario are gained; conversely, the SBO scenario does it for a high-pressure and high-steam fraction (late operation of sprays, though, might drastically change it).

By conducting a separate containment analysis, computation times were substantially reduced, enabling comparison of the simulation results with those from other codes employed within the EU AMYHCO project.

The results presented in the previous sections lead to the following observations related to the scenarios' features:

- PARs efficiently reduce the concentration of combustible gases and oxygen in the containment atmosphere. The latter might play a key role in the ex-vessel phase, turning a flammable mixture into an inflammable one. Scenarios with late vessel failure, like SBOs, would favor reaching oxygen-depleted atmospheres (<5% molar).
- In case of steam-starved scenarios, like LBLOCAs, the ex-vessel phase represents a challenge for a PAR system. In particular, if the reactor vessel fails early in the accident, PARs will not have enough time to extensively consume the oxygen in the containment atmosphere

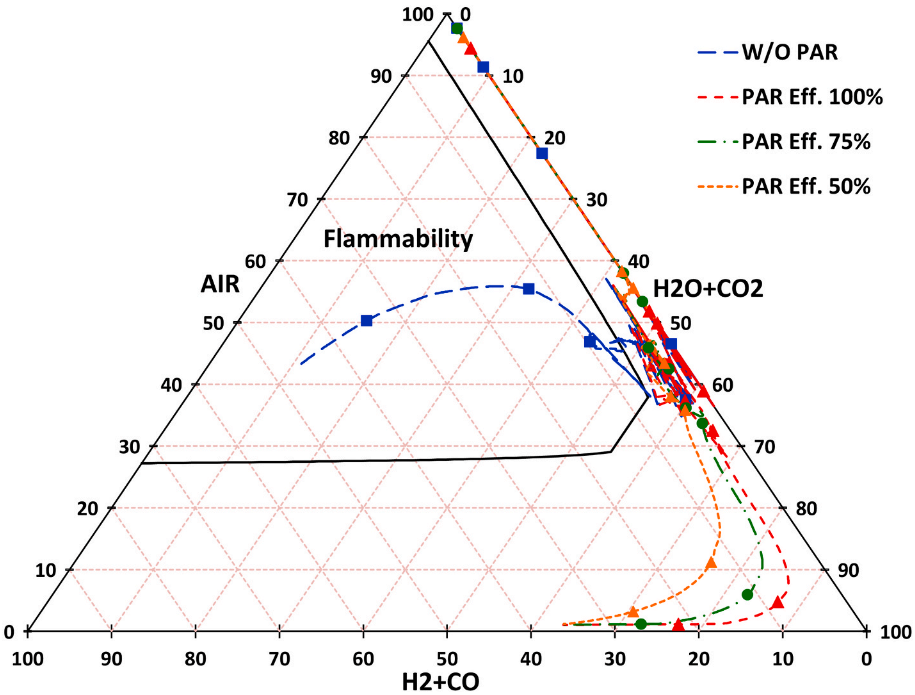


**Fig. 8.** Shapiro diagram in the annular-east atmosphere for the SBO. Comparison of PAR's efficiency.

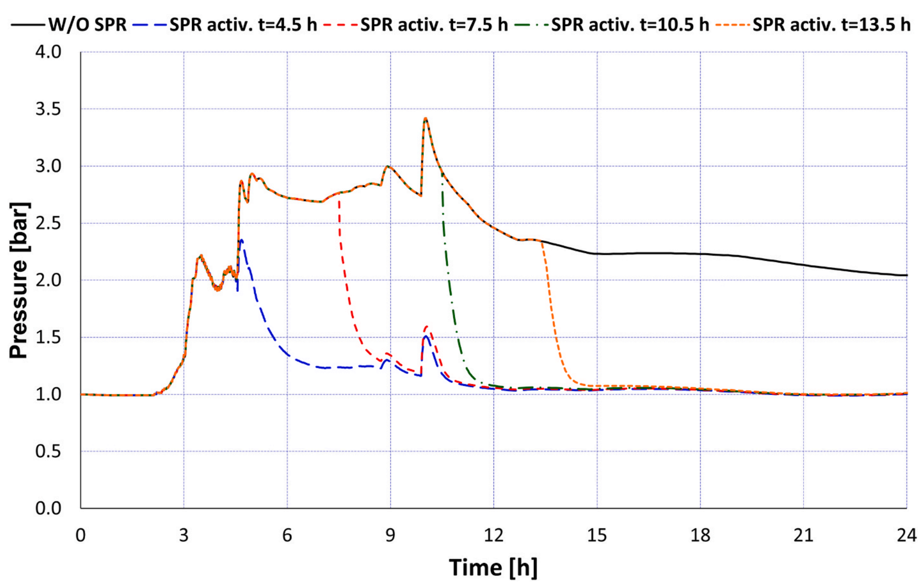


**Fig. 9.** Containment pressure evolution for the SBO sequence. Comparison of spray activation time in siliceous concrete.

before additional $H_2$ and CO are continuously released by the MCCI. Given the significance of the ex-vessel phase in combustion risk, the availability of suitable validated correlations for $H_2$-CO mixtures under oxygen-lean conditions is fundamental to this kind of analysis.

- High steam fraction during accidents implies the gas mixture dilution with a low molar fraction of combustible gases. Given that the PAR recombination model adopted is not explicitly affected by the presence of steam, steam-rich conditions would be preferable without compromising combustible-gas mitigation, provided there is sufficient margin up to the design pressure.

The comparison of both sequences during in- and ex-vessel phases shows how $H_2$/CO mitigation effectiveness is strongly sequence-dependent and a single strategy should not be assumed for all scenarios.

As for management actions, the following insights are identified:

- PAR's reliability is sound. Even when the full PAR system capacity is reduced to half, the effect of PARs is evident and quantitative. The reason underneath is the dependence of the recombination rate on combustible gas concentration. Nonetheless, a large generation of combustible gas in the ex-vessel phase may lead to the formation of flammable gas mixtures within the containment.
- Recovery of cooling systems initially unavailable during the accident should not lead to their automatic activation. In case of prolonged in-vessel phases, a delayed onset of their operation beyond 7.5 h is recommended, so that PARs operate long enough to consume at least three-fourths of the oxygen initially present in the containment atmosphere.

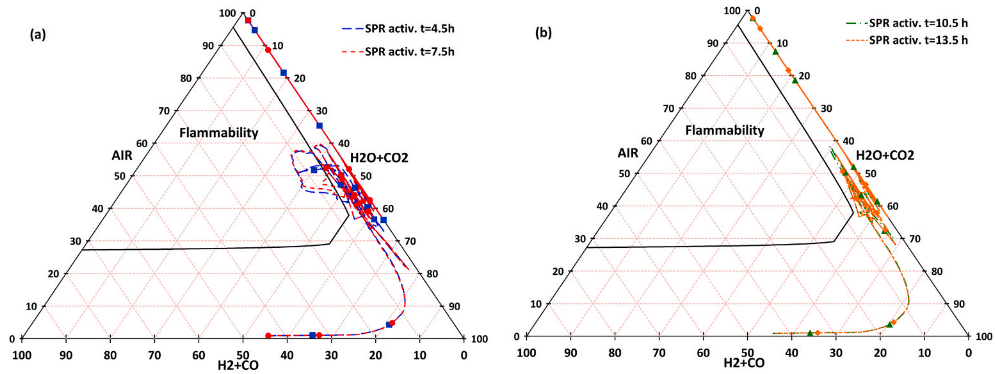


**Fig. 10.** Shapiro diagram in the annular-east atmosphere for the SBO sequence. Comparison of spray activation time in siliceous concrete.

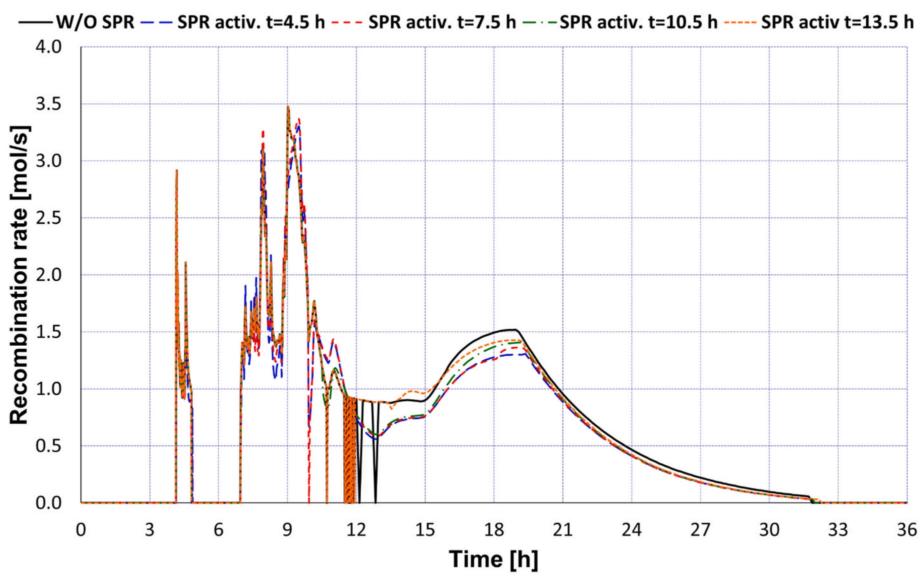


**Fig. 11.** Total recombination rate in the annular-east compartment. Comparison of spray activation time in siliceous concrete.

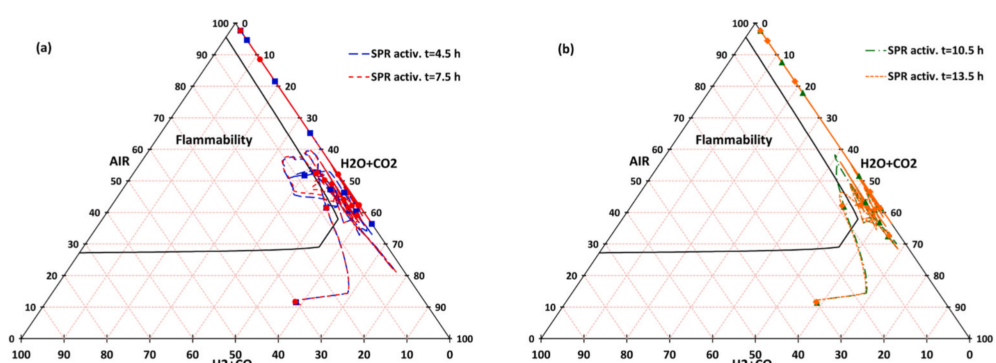


**Fig. 12.** Shapiro diagram in the annular-east atmosphere for the SBO sequence. Comparison of spray activation time in limestone concrete.

- Although particular results are scenario-specific, generally, the eventual depletion of oxygen in the containment allows the cooling system to be activated without increasing the risk for combustion. Nonetheless, if a rapid containment pressure rise to values close to the design pressure occurs, lowering the containment pressure might take priority.
- With the postulated assumptions on mitigation systems availability (PARs), large masses of combustible gases can accumulate in the containment in the long term of the sequence due to oxygen starvation. In case of initiating the FCVS, attention should be given to where this in-containment gas mixture will come into contact with oxygen-rich environmental air and where it could re-establish flammable conditions.

It is worth noting that the results obtained represent upper bounds under the conservative assumptions adopted and are not representative of typical PWR sequences.

Finally, the performed analyses show that any PAR system design and distribution should consider both the in-vessel and the ex-vessel phases. Thereby, particularly, the basement concrete composition has a strong impact on the composition of generated gases.

## CRediT authorship contribution statement

**Joan Fontanet:** Data curation, Formal analysis, Investigation, Methodology, Visualization, Writing – original draft, Writing – review & editing. **Luis E. Herranz:** Formal analysis, Funding acquisition, Investigation, Methodology, Visualization, Writing – review & editing.

## Declaration of competing interes

The authors declare that they have no known competing financial interests or personal relationships that could have appeared to influence the work reported in this paper.

## Acknowledgment

The AMHYCO project, coordinated by the UPM (Universidad Politécnica de Madrid) has received funding from the Euratom research and training programme 2019-2020 under Grant Agreement n°945057. The content of this paper reflects only the authors' view. The European Commission is not responsible for any use that may be made of the information it contains.

MELCOR code is an integral severe accident code developed by Sandia National Laboratory (SNL). It is used at CIEMAT thanks to the CSARP agreement of SNL with the Spanish Regulatory Body (Consejo de Seguridad Nuclear – CSN).

The authors acknowledge the IRSN (ASNR at present), particularly to Ahmed Bentaib, Alexandre Bleyer, and Ludovic Maas for simulating and providing source data for the SBO sequence within the AMHYCO project.

## References

[1] Chapter 3 - early containment failure, in: B.R. Sehgal (Ed.), Nuclear Safety in Light Water Reactors, Academic Press, Boston, 2012, pp. 185–306, https://doi.org/10.1016/B978-0-12-388446-6.00003-4.

[2] TEPCO, Evaluation of the Situation of Cores and Containment Vessels of Fukushima Daiichi Nuclear Power Station Units-1 to 3 and Examination into Unsolved Issues in the Accident Progression, Progress Report No. 3, 2015.

[3] A. Bentaib, N. Meynet, A. Bleyer, Overview on hydrogen risk research and development activities: methodology and open issues, Nucl. Eng. Technol. 47 (2015) 26–32, https://doi.org/10.1016/j.net.2014.12.001.

[4] IAEA, Mitigation of Hydrogen Hazards in Severe Accidents in Nuclear Power Plants, IAEA, Viena (Austria), 2011.

[5] NEA/CSNI, Status Report on Hydrogen Management and Related Computer Codes, 2014.

[6] D. Magallon, A. Mailliat, J.-M. Seiler, K. Atkhen, H. Sjövall, S. Dickinson, J. Jakab, L. Meyer, M. Buerger, K. Trambauer, L. Fickert, B.R. Sehgal, Z. Hozer, J. Bagues, F. Martin-Fuentes, R. Zeyen, A. Annunziato, M. El-Shanawany, S. Guentay, C. Tinkler, B. Turland, L.E.H. Puebla, European expert network for the reduction of uncertainties in severe accident safety issues (EURSAFE), Nucl. Eng. Des. 235 (2005) 309–346, https://doi.org/10.1016/j.nucengdes.2004.08.042.

[7] D. Manara, D. Jacquemain, J.P. Van Dorsselaere, P.D. Bottomley, M. Adorni, C. Journeau, Y. Pontillon, T. Lind, L.E. Herranz, F. Rocchi, A. Schaffrath, J.C. de la Rosa, S. Bechta, J. Duspiva, I. Kljenak, P. Dejardin, Severe accident research priority ranking: a new assessment wight years after the Fukushima daiichi accident, in: Proceedings of the European Review Meeting on Severe Accident Research, Prague (Czech Republic), 2019.

[8] ENSREG, Peer review report, Stress Tests Performed on European Nuclear Power Plants, 2012.

[9] IAEA, Considerations on the Application of the IAEA Safety Requirements for the Design of Nuclear Power Plants, 2016.

[10] F. Arnould, E. Bachellerie, M. Aglaire, B. de Boeck, O. Braillard, B. Eckardt, F. Ferroni, R. Moffett, G. Van Goethem, State of Art on Hydrogen Passive Autocatalitic Recombiner, In: Nice (France), 2001.

[11] G. Jiménez, L.E. Herranz, A. Bentaib, C. Nabiha, E.A. Reinecke, S. Kelm, M. Loeffler, M. Braun, C. Bratfisch, I. Kljenak, O. Sevbo, D.C. Visser, Z. Liang, S. Balech, AMHYCO project – towards an enhanced accident management of the H2/CO combustion risk, in: The 19th International Topical Meeting on Nuclear Reactor Thermal Hydraulics (NURETH-19), Brussels (Belgium), 2022.

[12] S. Kelm, M. Klauck, C. Vázquez-Rodríguez, G. Jiménez, L. Serra, A. Domínguez-Bugarín, L.E. Herranz, J. Fontanet, L. Vitores, A. Bentaib, L. Maas, A. Bleyer, N. Chaumeix, M. Braun, J. Hoffrichter, M. Müer, I. Kljenak, O. Sevbo, A. Iskra, F.S. L. (Fajar) Pangukir, D.C. (Dirk) Visser, Z. (Rita) Liang, Detailed assessment of combustion risk and PAR efficiency in the late phase of a severe accident within the European AMHYCO project, Nucl. Eng. Des. 446 (2026) 114588, https://doi.org/10.1016/j.nucengdes.2025.114588.

[13] L.L. Humphries, B.A. Beeny, F. Gelbard, T. Haskin, D.L. Louie, J. Phillips, J. Reynolds, R.C. Schmidt, MELCOR Computer Code Manuals Vol. 2: Reference Manual Version 2.2.r2023, Sandia National Laboratories, Albuquerque, 2023.

[14] H.T. Kim, J. Kim, MELCOR analysis of a SPARC experiment for Spray-PAR interaction during a hydrogen release, Energies 13 (2020), https://doi.org/10.3390/en13215696.

[15] E.A. Reinecke, J. Fontanet, L.E. Herranz, Z. Liang, L. Maas, O. Mazurok, J.S. Park, D.C. Visser, M. Hupp, S. Gupta, PAR model development exercise in the framework of SAMHYCO-NET, Nucl. Eng. Des. 399 (2022) 112035, https://doi.org/10.1016/J.NUCENGDES.2022.112035.

[16] J. Fontanet, L.E. Herranz, Assessment of the AREVA's formulation of PARs recombination rate, in: Proceedings - 19th International Topical Meeting on Nuclear Reactor Thermal Hydraulics (NURETH-19), Brussels (Belgium), 2022. Log nr.: 35419.

[17] S Kelm, M. Klauck, S. Beck, H.-J. Allelein, G. Preusser, M. Sangiorgi, W. Klein-Hessling, I. Bakalov, A. Bleyer, A. Bentaib, I. Kljenak, M. Stempniewicz, P. Kostka, S. Morandi, B. Ada Del Corno, C. Bratfisch, T. Risken, L. Denk, Z. Parduba, S. Paci, A. Manfredini, A. Silde, P. Juris, J. Jancovic, H.G. Lele, S. Ganju, Generic containment: detailed comparison of containment simulations performed on plant scale, Ann. Nucl. Energy 74 (2014) 165–172, https://doi.org/10.1016/j.anucene.2014.07.006.

[18] M. Di Giuli, S. Yu, A.M. Swaidan, M. Barbion, P. Foucaud, C. Etienne, P. Dejardin, MELCOR 2.2-ASTEC V2.2 crosswalk study reproducing SBLOCA and CSBO scenarios in a PWR1000-like reactor part II: analysis of containment thermal-hydraulics and ex-vessel phenomena, Nucl. Eng. Des. 403 (2023) 112150, https://doi.org/10.1016/j.nucengdes.2022.112150.

[19] F. Mascari, NUREG/IA-0515, "Analyses of an Unmitigated Station Blackout Transient in a Generic PWR-900 with ASTEC, MAAP and MELCOR Codes," (n.d.).

[20] N. Zhao, Y. Chen, W. Ma, S. Bechta, P. Isaksson, A nodal sensitivity study of MELCOR simulation for severe accidents in a pressurized water reactor, Ann. Nucl. Energy 160 (2021) 108373, https://doi.org/10.1016/j.anucene.2021.108373.

[21] P. Omidifard, A. Pirouzmand, K. Hadad, J. Rezaee, Investigating the effect of spray system on the containment condition of VVER1000/V446 NPP during LBLOCA and TLOFW accidents, Nucl. Eng. Des. 413 (2023) 112562, https://doi.org/10.1016/j.nucengdes.2023.112562.

[22] L.E. Herranz, J. Fontanet, D2.2 – Identification and Analysis of Accident Sequences Posing High H2/CO Combustion Risk (PWR-W, PWR-VVER, PWR-KWU), UC-Euratom, 2023.

[23] L.E. Herranz, J. Fontanet, M. Braum, A. Bleyer, A. Bentaib, L. Maas, I. Kljenak, M. Leskovar, M. Müer, J. Hoffrichter, M.K. Koch, High combustion risk sequences. Identification and characterization, in: 10th European Review Meeting on Severe Accident Research (ERMSAR2022), Karlsruhe (Germany), 2022.

[24] L. Serra, A. Domíngues-Bugarín, C. Vázquez-Rodríguez, G. Jiménez, D2.1 – Data for the Generic Containment Analysis (PWR-W, PWR-VVER, PWR-KWU), UC-Euratom, 2023.

[25] European Committee for Standardization, Eurocode 2: Design of Concrete Structures - Part 1-2: General Rules - Structural Fire Design, 2004.

[26] E. Bachellerie, F. Arnould, M. Auglaire, B. de Boeck, O. Braillard, B. Eckardt, F. Ferroni, R. Moffett, Generic approach for designing and implementing a passive autocatalytic recombiner PAR-system in nuclear power plant containments, Nucl. Eng. Des. 221 (2003) 151–165, https://doi.org/10.1016/S0029-5493(02)00330-8.

[27] E.A. Reinecke, A. Bentaib, S. Kelm, W. Jahn, N. Meynet, C. Caroli, Open issues in the applicability of recombiner experiments and modelling to reactor simulations, Prog. Nucl. Energy 52 (2010) 136–147, https://doi.org/10.1016/j.pnucene.2009.09.010.

[28] M. Braun, E.-A. Reinecke, AMHYCO engineering correlation to describe the conversion of flammable gases in framatome passive autocatalytic recombiners, Nucl. Eng. Des. 442 (2025) 114206, https://doi.org/10.1016/j.nucengdes.2025.114206.

[29] NEA/CSNI, Core Exit Temperature (CET) Effectiveness in Accident Management on Nuclear Power Reactor, 2010.

[30] Chapter 6 - severe accident management, in: B.R. Sehgal (Ed.), Nuclear Safety in Light Water Reactors, Academic Press, Boston, 2012, pp. 519–588, https://doi.org/10.1016/B978-0-12-388446-6.00006-X.